Nonlinear electrophoresis of dielectric particles in Newtonian fluids

Joseph Bentor,[1] Heston Dort,[1] Rajan Ashutosh Chitrao,[1] Youwei Zhang,[2] and Xiangchun Xuan[1]

[1]Department of Mechanical Engineering, Clemson University, Clemson, SC 29634-0921, USA

[2]Shanghai Diecheng Photoelectronics Technology Co., Ltd, Shanghai, China 201800

Correspondence: Prof. Xiangchun Xuan, Department of Mechanical Engineering, Clemson University, Clemson, SC 29634-0921, USA. **E-mail:** xcxuan@clemson.edu

Abstract

In classical electrokinetics the electrophoretic velocity of a dielectric particle is a linear function of the applied electric field. Theoretical studies have predicted the onset of nonlinear electrophoresis at high electric fields because of the non-uniform surface conduction over the curved particle. However, experimental studies have been left behind and are insufficient for a fundamental understanding of the parametric effects on nonlinear electrophoresis. We present in this work a systematic experimental study of the effects of buffer concentration, particle size, and particle zeta potential on the electrophoretic velocity of polystyrene particles in a straight rectangular microchannel for electric fields of up to 3 kV/cm. The measured nonlinear electrophoretic particle velocity is found to exhibit a 2(±0.5)-order dependence on the applied electric field, which appears to be within the theoretically predicted 3- and 3/2-order dependences for low and high electric fields, respectively. Moreover, the obtained nonlinear electrophoretic particle mobility increases with decreasing buffer concentration (for the same particle) and particle size (for particles with similar zeta potentials) or increasing particle zeta potential (for particles with similar sizes). These observations are all consistent with the theoretical predictions for high electric fields.

Keywords

Electrokinetics / Surface conduction / Electrophoresis / Microfluidics

1 Introduction

Electrophoresis is an electrokinetic phenomenon widely adopted for particle transport and manipulation in micro- and nano-fluidic devices [1-3]. It is the movement of an electrically charged particle relative to the suspending fluid (either Newtonian [4,5] or non-Newtonian [6,7]) in response to an imposed electric field, which results from the Coulomb force acting on the net charge inside the electric double layer (EDL) formed at the fluid-particle interface [8,9]. In classical electrokinetics, the electrophoretic velocity, V_{ep}, of a non-polarizable dielectric particle in an unbounded Newtonian fluid exhibits a linear dependence on the electric field, E, and particle zeta potential, ζ_p, via the Smoluchowski equation under the thin EDL limit [10,11],

$$V_{ep} = \frac{\varepsilon\zeta_p}{\eta}E \qquad (1)$$

where ε is the fluid permittivity and η is the fluid viscosity. However, recent studies indicate that the linearity for V_{ep} is valid only in the limit of a weak electric field, $\beta = Ea/\phi \leq 1$, and a small particle zeta potential, $\zeta_p/\phi < 1$, where a is the particle radius and ϕ is the thermal voltage. Under these conditions, the ions within the EDL of the particle can maintain the equilibrium state yielding a homogeneous electrostatic potential and ionic concentration [12-14].

Increasing the electric field and/or particle zeta potential distorts the EDL and induces ionic fluxes across the EDL because of the surface conduction effect [15-18], leading to a nonlinear dependence of V_{ep} on both E and ζ_p [19-22],

$$V_{ep} = \mu_{ep}^{(1)}E + \mu_{ep}^{(3)}E^3 \qquad (2)$$

$$\mu_{ep}^{(3)} \sim Du \frac{\varepsilon a^2}{\eta \phi} \tag{3}$$

$$Du = \frac{2sinh(\zeta_p/2\phi)}{\kappa a}(1 + 2\alpha^-) \tag{4}$$

where $\mu_{ep}^{(1)}$ is the linear electrophoretic particle mobility, $\mu_{ep}^{(3)}$ is the nonlinear electrophoretic particle mobility, Du is the Dukhin number characterizing the surface conduction effect, κ is the inverse of the Debye length, and α^- is the dimensionless drag coefficient for counter-ions. The formula for $\mu_{ep}^{(3)}$ in Eq. (3) was obtained by Schnitzer and Yariv [23] for $Du \ll 1$ at small Peclet numbers, $Pe = \varepsilon \zeta_p E a/\eta D \ll 1$, where D is the effective diffusion coefficients of ions. A similar formula to Eq. (3) was also reported by Mishchuk and Dukhin [24] while a slightly different formula was later obtained by Shilov et al. [25] for arbitrary values of Du. Schnitzer et al. [21] also obtained an expression for $\mu_{ep}^{(3)}$ in the weak-field limit, $\beta \leq 1$, for arbitrary values of Du, which, however, shows inconsistencies with that from Shilov et al. [25] because of the ignored ion advection and other salt related effects in the latter. In all these formulae except that from Schnitzer et al. [21], $\mu_{ep}^{(3)}$ increases with increasing Du that may be a consequence of the increasing Debye length, $1/\kappa$, via the decrease of buffer concentration or the increasing particle zeta potential. It also increases with the particle radius, a, even though Du itself actually gets smaller for larger particles. At large Peclet numbers, $Pe \gg 1$, or equivalently strong electric fields, $\beta \gg 1$, Schnitzer & Yariv [23] predicted an $E^{3/2}$ dependent nonlinear electrophoretic particle velocity,

$$V_{ep} = \mu_{ep}^{(1)} E + \mu_{ep}^{(3/2)} E^{3/2} \tag{5}$$

$$\mu_{ep}^{(3/2)} \sim f(\zeta_p) Du \frac{\varepsilon \phi^2 a^{1/2}}{\eta (\zeta_p)^{3/2}} \sim f(\zeta_p) \frac{sinh(\zeta_p/2\phi)}{\kappa a^{1/2} (\zeta_p)^{3/2}} \tag{6}$$

where $f(\zeta_p)$ is a function of ζ_p. Therefore, $\mu_{ep}^{(3/2)}$ increases with the increase of particle zeta potential or the decrease of buffer concentration and particle size. Mishchuk and Dukhin [24] reported a different formula for $\mu_{ep}^{(3/2)}$, which decreases with the increase of particle zeta potential. Other theoretical and numerical studies on nonlinear particle electrophoresis can be referred to a recent review article from Khair [26].

There have also been a few experimental studies on nonlinear electrophoresis of dielectric particles. The earliest experiment seems to be reported by Kontush et al. [27] in a Russian colloidal journal that is unfortunately not accessible to the authors of this work. However, Mishchuk and Dukhin [24] noted that the prediction of $\mu_{ep}^{(3/2)}$ in Eq. (6) agrees closely with the experimental result of Kontush et al. [27] for spherical latex particles. Shilov et al. [25] measured the lateral drift of sedimenting polystyrene particles of 30 μm diameter in water and KCl solution under electric pulses. Their observed cubic electrophoresis for electric fields stronger than 0.1 kV/cm agrees with the theoretical prediction of $\mu_{ep}^{(3)}$ in Eq. (3). Later, Barany [28] reported the measurement of polymer-coated polystyrene particles using the same experimental setup as in Shilov et al. [25], where the cubic electrophoresis is found as theoretically predicted to increase with the particle diameter. Mishchuk and Barninova [29] also observed a greater nonlinear electrophoretic velocity for larger latex particles for electric fields of up to 0.2 kV/cm, in line with the prediction of $\mu_{ep}^{(3)}$ in Eq. (3). In contrast, the nonlinear electrophoretic velocity of larger latex particles was found smaller for larger electric fields of up to 0.8 kV/cm, corresponding to the theoretical prediction of

$\mu_{ep}^{(3/2)}$ in Eq. (6) though the Peclet number was reported to remain on the order of 1 in both experiments.

In another study, Youssefi and Diez [30] measured the electrophoretic velocity of carboxyl treated 0.2 μm diameter polystyrene particles for electric fields over the range of 0.1 to 250 kV/cm. They observed a 3/2-order dependence of their electrophoresis measurements on electric fields of up to 40 kV/cm, in agreement with the prediction of Eq. (6). For even higher electric fields, their measured electrophoretic velocity still increases with the electric field but slower than the 3/2-order dependence. Tottori et al. [31] studied the electrophoretic motion of highly charged polystyrene and poly(methyl methacrylate) (PMMA) particles of 0.5 μm diameter for electric fields of up to several kV/cm. Their measured nonlinear electrophoretic velocity exhibits a 3-order dependence on the imposed electric field, in good agreement with the theoretical prediction of Eq. (3). In a more recent study, Cardenas-Benitez et al. [32] reported a reversed electrokinetic motion for carboxylated polystyrene particles of 1.0, 1.9, and 5.1 μm diameters in dilute KCl solutions when the imposed electric field is beyond a threshold magnitude (smaller than 1 kV/cm for all cases). The authors termed this state the electrokinetic equilibrium condition (EEC) and explained it using the nonlinear electrophoretic particle velocity in Eq. (2) that increases more quickly with the electric field than the opposing linear electroosmotic fluid velocity. They later used the EEC to obtain the nonlinear electrophoretic mobilities of other types of particles [33,34] and achieve the separation of almost identical particles [35] as well as sub-100 V particle trapping [36].

However, the current experimental studies are still insufficient for a systematic understanding of the parametric effects of fluid and particle properties on nonlinear electrophoresis. We carry out a set of experiments in this work to investigate the respective effects of buffer concentration, particle size, and particle zeta potential on the nonlinear electrophoretic velocity of dielectric particles in aqueous electrolyte solutions through a straight rectangular microchannel. Specifically we will study if and how the nonlinear electrophoretic particle mobility, $\mu_{ep}^{(n)}$, and nonlinear index, $n \neq 1$, vary with each of these fluid and particle properties.

2 Materials and methods

2.1 Microchannel and chemicals

The microchannel was fabricated from polydimethylsiloxane (PDMS) with the standard soft lithography technique [37]. The channel is straight and 1 cm long with a uniform width and depth of 50 μm each. The experiment studies the effects of three individual parameters on nonlinear particle electrophoresis. The first parameter is buffer concentration, for which 5 μm diameter plain polystyrene particles (Sigma-Aldrich) were re-suspended in phosphate buffer solutions with concentrations ranging from 0.01 to 0.05, 0.075 and 0.1 mM. These solutions were all prepared by diluting the original 50 mM buffer solution (pH = 7) with DI water. The second parameter is particle size, for which 3 μm, 5 μm and 10 μm diameter plain polystyrene particles (Sigma-Aldrich) were each re-suspended in 0.075 mM phosphate buffer. The third parameter is particle zeta potential, for which three types of (nearly) 5 μm diameter polystyrene particles, including 5 μm plain particles from Sigma-Aldrich, 4.95 μm fluorescent carboxyl particles from Bangs Laboratories, and 4.8 μm fluorescent carboxylate-modified particles from Thermo-Scientific, were each re-suspended in 0.075 mM phosphate buffer. These particles were noticed to travel at different speeds in the same solution under the same electric field, indicating that they have dissimilar zeta potentials probably because of their intrinsic surface groups.

2.2 Experimental technique

The prepared particle suspensions were each driven through the microchannel by a high-voltage DC power supply (Glassman High Voltage) via platinum electrodes inserted into the end-channel reservoirs. The voltages varying from 0.1 to 3 kV were imposed upon the 1 cm long channel, yielding the average electric fields of 0.1 to 3.0 kV/cm. The corresponding dimensionless electric field, $\beta = Ea/\phi$, for $a = 2.5$ μm particles was calculated to range from 1 to 30. For each applied voltage, the direction of electric field was reversed once via a two-way electric switch to repeat the test for the purpose of canceling the potential influence of backflow. Moreover, each run of test was kept no more than 30 s (i.e., 15 s for each direction) to minimize both the backflow [38] and Joule heating effects [39]. In addition, the reservoirs were intentionally made large to minimize the impact of pH change due to electrolysis at high electric fields, which also facilitates reducing the backflow. The motion of particles was observed to remain along the direction of the applied electric field, indicating stronger fluid electroosmosis (which is along the electric field direction) than particle electrophoresis (which is against the electric field direction) in all tested cases. It was recorded using an inverted microscope imaging system (Nikon Eclipse TE2000U, Nikon Instruments). The CCD camera (Nikon DS-Qi1Mc) was run in a binning mode for increasing the frame rate to around 50 fps at a reduced concentration. The captured images were processed using the Nikon imaging software (NIS-Elements AR 2.30).

The velocity of particles was measured using the particle tracking velocimetry, where 3-5 particles traveling along the channel centerline (only) were tracked to obtain an average value. To quantify the effect of the potential pressure-driven backflow at high electric fields, we seeded 1 μm diameter polystyrene particles (Bangs Laboratories) into the reference solution, i.e., 0.075 mM buffer, for a real-time recording of the fluid velocity immediately after the electric field was turned off. The measured velocity of the tracer particles along the channel centerline was found no more than 5% of that of our test particles under the highest electric field. We also monitored the temporal variation of electric current in the highest-concentration 0.1 mM buffer for estimating the Joule heating effects and the accompanying electrothermal flow [39]. The electric current rise was found to remain less than 10% of the initial value within 15 s application of the highest 3 kV/cm electric field, indicating a fewer than 5 °C increase in the average fluid temperature for an assumed 2% temperature coefficient of the electric conductivity [40]. This small temperature elevation was assumed to have an insignificant impact on the fluid properties and hence the particle motion. In addition, we estimated that under pure DC electric fields the induced charge electroosmotic flow at the reservoir-microchannel junction [39] is weak with no significant influence on the particle motion inside the microchannel.

2.3 Experimental data analysis

The measured particle velocity, V_p, in the straight microchannel is the sum of the electroosmotic fluid velocity, V_{eo}, and electrophoretic particle velocity,

$$V_p = V_{eo} + V_{ep} \tag{7}$$

We split V_{ep} into the linear component, $V_{ep}^{(1)}$, and the nonlinear component, $V_{ep}^{(n)}$, where the nonlinear index, $n > 1$. Thus, the measured particle velocity can be rewritten as,

$$V_p = V_{ek} + V_{ep}^{(n)} \tag{8}$$

$$V_{ek} = V_{eo} + V_{ep}^{(1)} = \mu_{ek} E \tag{9}$$

$$V_{ep}^{(n)} = \mu_{ep}^{(n)} E^n \tag{10}$$

where V_{ek} is the electrokinetic particle velocity that has been long accepted to scale linearly with the applied electric field in classical electrokinetics [9,12], μ_{ek} is the (linear) electrokinetic particle mobility [11, 14], and $\mu_{ep}^{(n)}$ is the nonlinear electrophoretic particle mobility. The primary objective of this work is to study if and how $\mu_{ep}^{(n)}$ and n vary with the fluid and particle properties. To do so, we utilize the same method as in Tottori et al. [31] to extract $V_{ep}^{(n)}$ from the experimental data. Briefly, the linear electrokinetic particle velocity, V_{ek}, was determined through a linear fit (the slope denotes the electrokinetic particle mobility, μ_{ek}) of the measured particle velocity, V_p, at the three smallest electric fields, i.e., 0.1, 0.2 and 0.25 kV/cm. This analysis was based on the assumption that $V_{ep}^{(n)} \ll V_{ek}$ and hence $V_p \cong V_{ek}$ at small electric fields. The nonlinear electrophoretic particle velocity, $V_{ep}^{(n)}$, was then calculated by subtracting the obtained V_{ek} from the measured V_p. The log-log transformation was then used to determine the nonlinear electrophoretic particle mobility, $\mu_{ep}^{(n)}$, and nonlinear index, n, via the intercept and slope of the linear fit for $V_{ep}^{(n)}$ as a function of E.

3 Results and discussion

3.1 Effect of buffer concentration

Figure 1 plots the experimentally measured velocities of 5 μm-diameter Sigma-Aldrich particles in buffer solutions with concentration varying from 0.01 to 0.05, 0.075 and 0.1 mM under different electric fields. The error bars (note some of them are within the symbol size and become invisible) highlight the maximum variations of the measured of 3-5 particle velocities with respect to their average for each electric field. The measured particle velocity, V_p, in each buffer solution is observed to increasingly deviate from the linear electrokinetic particle velocity, V_{ek} (reflected by the linear trendlines in Fig. 1), at higher electric fields. This upward trend goes against that reported by Cardenas-Benitez et al. [32], the reason behind which is currently unclear. One possible explanation could be that the electrophoretic particle velocity, V_{ep}, in our experiment decreases nonlinearly with the increase of electric field because of, for example, the predicted retardation effect of surface conduction [23] and/or dielectric-solid polarization at strong fields [43]. We will work on revising the experimental technique to obtain V_{ep} directly. The discrepancy between V_p

and V_{ek}, i.e., the nonlinear electrophoretic particle velocity, $V_{ep}^{(n)}$, exhibits an apparent dependence on the buffer concentration in Fig. 1. The Peclet number in this experiment was estimated to vary from around 2 to 60 using $Pe = V_p a/D$ based on the effective diffusion coefficient, $D = 0.5 \times 10^{-9}$ m^2/s [41], and the average V_p of 0.4 and 12 mm/s for the lowest and highest electric fields of 0.1 and 3 kV/cm, respectively. This range of Pe covers both $1 < Pe < 10$ and $Pe \gg 1$, implying that $V_{ep}^{(n)}$ may be inclined towards $V_{ep}^{(3/2)}$ in Eq. (6).

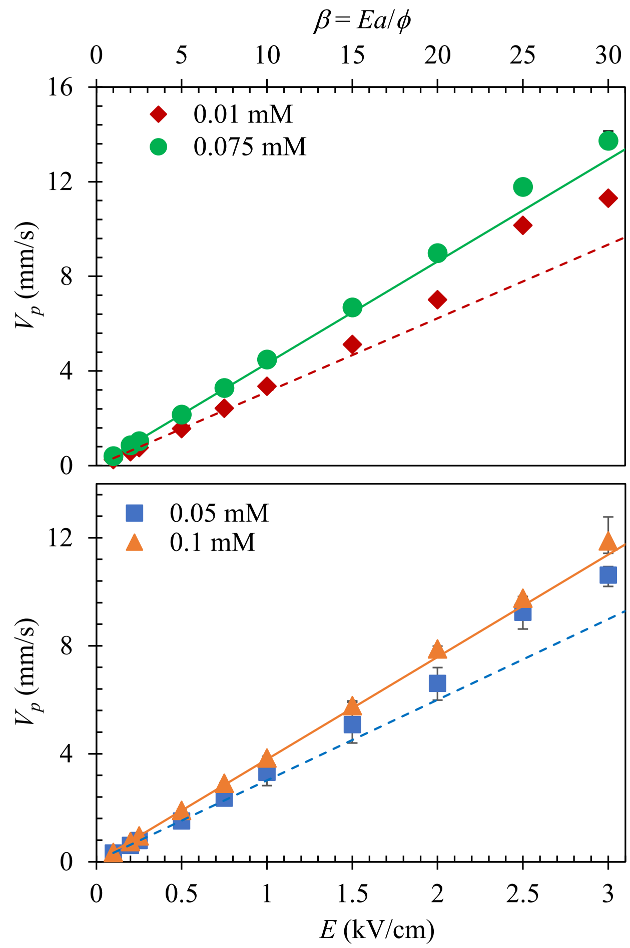

Figure 1. Experimentally measured (symbols with error bars) velocity, V_p, of 5 μm-diameter Sigma-Aldrich particles against electric field in 0.01, 0.05, 0.075 and 0.1 mM buffer solutions.

The solid and dashed lines are the linear fits of the experimental data points at the three smallest electric fields, representing the linear electrokinetic particle velocity, V_{ek}.

A summary of $V_{ep}^{(n)}$ in the four buffer solutions is shown in Fig. 2A as a function of the electric field. There is a clear trend that the nonlinear particle electrophoresis gets enhanced in lower-concentration buffers, which should be attributed to the thicker EDL therein (characterized by the Debye length, $1/\kappa$) and hence the stronger surface conduction effect. This trend is consistent with the predictions of both $\mu_{ep}^{(3)}$ in Eq. (3) and $\mu_{ep}^{(3/2)}$ in Eq. (6) in terms of the increased Dukhin number, Du. The experimentally obtained data for $V_{ep}^{(n)}$ in each buffer solution are found to be best fitted with a positive power trendline as illustrated in Fig. 2A. We used the log-log transformation (see Fig. S-1 in the Supporting Information for the log-log plot) as noted above to determine the nonlinear electrophoretic particle mobility, $\mu_{ep}^{(n)}$, and nonlinear index, n, from the linear fit of $V_{ep}^{(n)}$ against E. Fig. 2B presents the extracted $\mu_{ep}^{(n)}$ and n that each exhibit a linear decreasing trend with the increase of buffer concentration. Specifically, the value of n decreases from approximately 2.4 in 0.01 mM buffer to 1.6 in 0.1 mM buffer, both of which appear to be within the theoretically predicted $n = 3$ and $3/2$ for small and large electric fields [23,24], respectively. The value of $\mu_{ep}^{(n)}$, whose unit is noted to vary roughly around $n = 2$, decreases from approximately 0.18 to 0.08 mm/(s·(kV/cm)^2) when the buffer concentration increases from 0.01 to 0.1 mM. As the change of buffer concentration often modifies the particle zeta potential [42], the observed trend for $\mu_{ep}^{(n)}$ may be associated with both factors. The sole effect of particle zeta potential will be discussed later in section **3.3**.

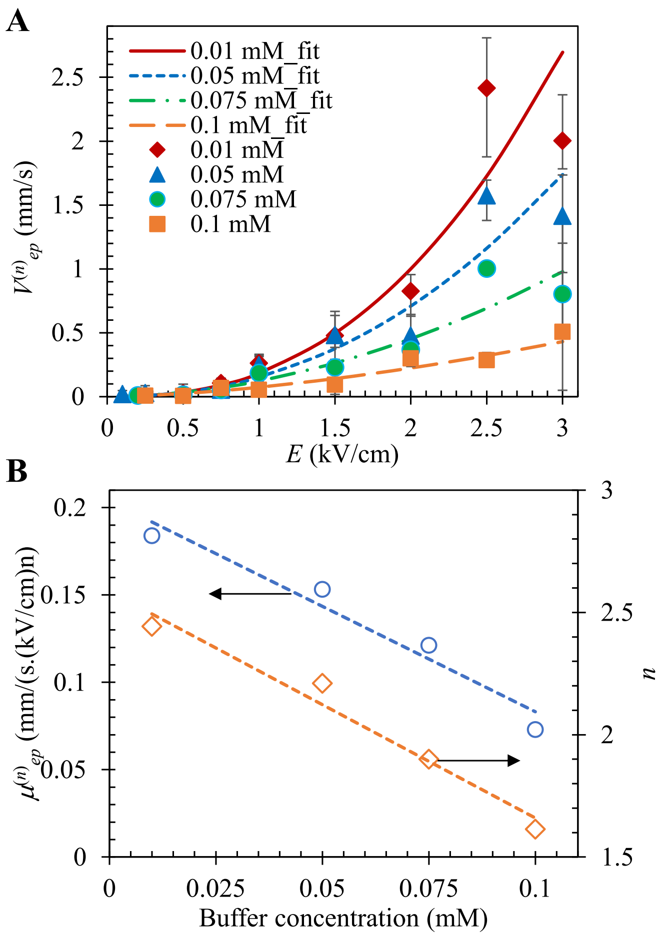

Figure 2. Nonlinear electrophoresis of 5 μm-diameter Sigma-Aldrich particles in 0.01, 0.05, 0.075 and 0.1 mM buffer solutions: (A) Experimentally obtained (symbols with error bars) nonlinear electrophoretic velocity, $V_{ep}^{(n)}$, as a function of electric field, where the curves are the positive power trendlines best fitted for the experimental data points; (B) Analytically extracted (symbols) nonlinear electrophoretic particle mobility, $\mu_{EP}^{(n)}$, and nonlinear index, n, from the power trendlines in (A) as a function of the buffer concentration, where the dashed lines are the linear fits for the analytical data points.

3.2 Effect of particle size

Figure 3 shows the experimentally measured velocities for 3 μm and 10 μm-diameter Sigma-Aldrich particles in 0.075 mM buffer solution. The electrokinetic particle velocity, V_{ek} (see the linear trendlines), is found insensitive to the particle size (including 5 μm), so is the electrokinetic particle mobility, $\mu_{ek} = 4.3 \times 10^{-8}$ m^2/V·s, and particle zeta potential. However, the deviation of the measured particle velocity, V_p, from V_{ek} is clearly greater for the smaller 3 μm particles. The estimated Peclet number spans from around 1.2 to 36 for 3 μm particles and from 4 to120 for 10 μm ones over the range of electric fields tested. Both ranges of Pe remain in the intermediate ($1 < Pe < 10$) and high ($Pe \gg 1$) regimes, and hence $V_{ep}^{(n)}$ should be also inclined towards $V_{ep}^{(3/2)}$ for 3 μm and 10 μm particles. The experimentally obtained nonlinear electrophoretic velocities, $V_{ep}^{(n)}$, for the three sizes of particles are compared in Fig. 4A, which shows a generally increasing trend with the decrease of particle diameter over the range of electric fields. They are again each best fitted with a positive power trendline, whose intercept and slope in the log-log space (see Fig. S-2 in the Supporting Information) gives the nonlinear electrophoretic particle mobility, $\mu_{ep}^{(n)}$, and nonlinear index, n, respectively. The extracted values of $\mu_{ep}^{(n)}$ and n both decrease with the increase of particle diameter, which are each best fitted with a negative power trendline as viewed in Fig. 4B.

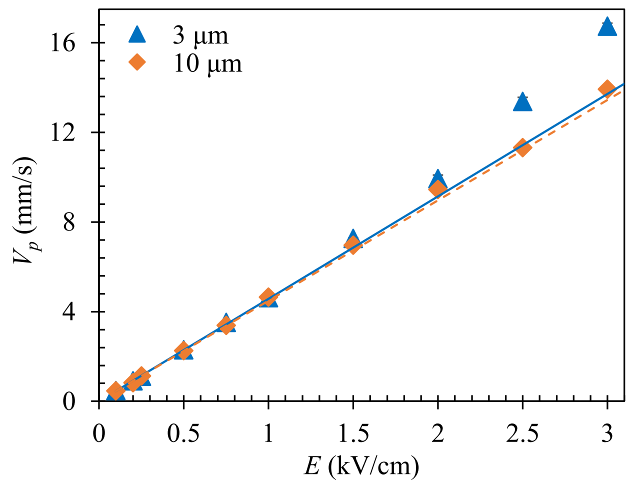

Figure 3. Experimentally measured (symbols with error bars) velocity, V_p, of 3 and 10 μm-diameter Sigma-Aldrich particles in 0.075 mM buffer solution at varying electric fields. The solid and dashed lines are the linear fits of the experimental data points at the three smallest electric fields, representing the linear electrokinetic particle velocity, V_{ek}.

It is noted from Eq. (4) that the Dukhin number, Du, get larger for smaller particles, which should yield stronger surface conduction effects. However, the theoretically predicted $\mu_{ep}^{(3)}$ in Eq. (3) for small Peclet numbers turns out to be a positive function of the particle diameter. Such a trend goes against our observation in Fig. 4B, where the value of $\mu_{ep}^{(n)}$ decreases from approximately 0.18 to 0.08 mm/(s·(kV/cm)^2) for assumed $n = 2$ when the particle diameter increases from 3 μm to 10 μm. It, however, appears consistent with the prediction of $\mu_{ep}^{(3/2)} \sim a^{-1/2}$ in Eq. (6) for large Peclet numbers because our estimated Pe are indeed more inclined towards the high regime as noted above. Moreover, the extracted range of $\mu_{ep}^{(n)}$ for particles of different sizes in Fig. 4B is found to match that in Fig. 2B for 5 μm particles in buffers of varying concentrations. In addition, our extracted value of n decreases from approximately 2.5 for 3 μm particles to 1.6 for 10 μm particles.

This range is also consistent with the experimentally obtained variation of n in Fig. 2B, and is again within that of the theoretically predicted $n = 3$ and $3/2$ for small and large electric fields [23,24], respectively.

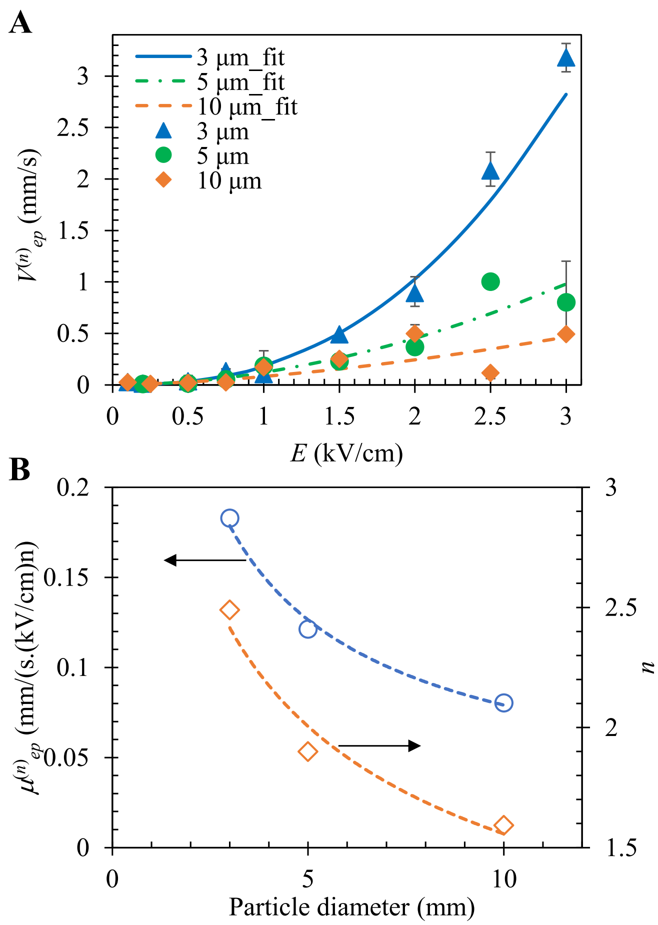

Figure 4. Nonlinear electrophoresis of 3, 5 and 10 µm-diameter Sigma-Aldrich particles in 0.075 mM buffer solution: (A) Experimentally obtained (symbols with error bars) nonlinear electrophoretic velocity, $V_{ep}^{(n)}$, as a function of electric field, where the curves are the positive power trendlines best fitted for the experimental data points; (B) Analytically extracted (symbols) nonlinear electrophoretic particle mobility, $\mu_{EP}^{(n)}$, and nonlinear index, n, from the power trendlines in (A) as a function of the particle diameter, where the dashed lines are the power fits for the analytical data points.

3.3 Effect of particle zeta potential

Figure 5 shows the experimentally measured velocities of 5 μm-diameter Thermo (Scientific) and Bangs (Laboratories) particles in 0.075 mM buffer solution. The electrokinetic velocity, V_{ek} (see the linear trendlines), of Thermo particles is smaller than that of Bangs particles, both of which are lower than that of Sigma (Aldrich) particles. The measured velocity, V_p, of Thermo particles shows a greater deviation from V_{ek} than that of Bangs particles, indicating stronger nonlinear electrophoresis. The estimated Peclet number is $1 \leq Pe \leq 43$ for Bangs particles and $0.6 \leq Pe \leq 50$ for Thermo particles over the range of electric fields tested. Therefore, the nonlinear electrophoretic velocities, $V_{ep}^{(n)}$, should be in theory inclined towards $V_{ep}^{(3/2)}$ for both types of particles. Fig. 6A compares the experimentally determined, $V_{ep}^{(n)}$, for the three types of particles, which are each best fitted with a positive power trendline. It is apparent that $V_{ep}^{(n)}$ grows larger with the decrease of V_{ek} over the range of electric fields, where the linear electrokinetic particle velocity, V_{ek}, as traditionally defined in Eq. (9), depends on the particle zeta potential via the following (linear) electrokinetic mobility, μ_{ek}, under the thin EDL limit [9,11,14],

$$\mu_{ek} = \frac{\varepsilon(\zeta_p - \zeta_w)}{\eta} \quad (11)$$

The wall zeta potential, ζ_w, for 0.075 mM buffer was found to be around −123 mV from the experimentally measured electroosmotic fluid velocity via the electric current monitoring method [44]. The particle zeta potential, ζ_p, was then calculated from Eq. (11) using the experimentally determined μ_{ek}.

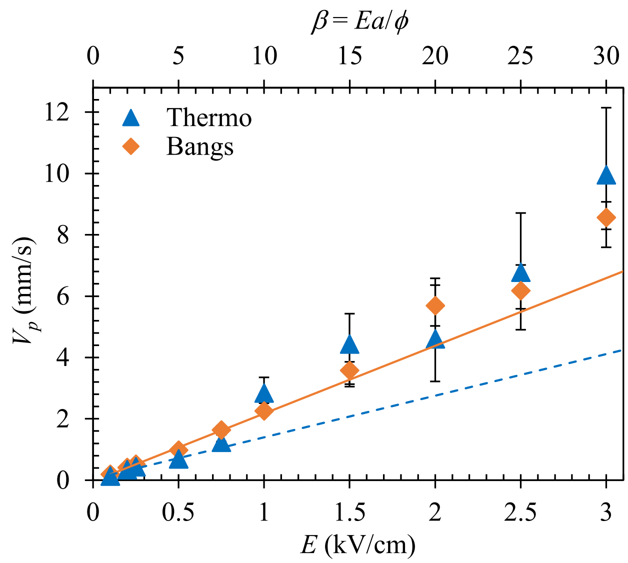

Figure 5. The experimentally measured (symbols with error bars) velocity, V_p, of 5 μm-diameter Thermo-Scientific and Bangs Laboratories particles in 0.075 mM buffer solution at varying electric fields. The solid and dashed lines are the linear fits of the experimental data points at the three smallest electric fields, representing the linear electrokinetic particle velocity, V_{ek}.

Figure 6B shows the extracted values of $\mu_{ep}^{(n)}$ and n as a function of $|\zeta_p|$ from the power trendlines in Fig. 6A (see Fig. S-3 in the Supporting Information for the log-log plot). The nonlinear index increases slightly from $n = 1.9$ for Sigma particles at $\zeta_p = -62.3$ mV to $n = 2.1$ for Thermo particles at $\zeta_p = -102.5$ mV. Accordingly, the nonlinear electrophoretic particle mobility increases quickly from $\mu_{ep}^{(n)} = 0.12$ to 0.55 mm/(s·(kV/cm)^2) (for assumed $n = 2$), where the data points can be fitted with a positive power trendline. Such an increasing trend with $|\zeta_p|$ for $\mu_{ep}^{(n)}$ seems consistent with the recent report of Tottori et al. [31] on the nonlinear electrophoresis of polystyrene and PMMA particles. It may be the consequence of the enhanced surface conduction effect as reflected by the increasing Dukhin number in the theoretical prediction of $\mu_{ep}^{(3/2)}$ in Eq.

(6) for high Peclet numbers. Specifically, the estimated value of Du [with $\alpha^- = 0.25$ in Eq. (4)], increases from 0.067 for Sigma particles to 0.14 and 0.16 for Bangs and Thermo particles, respectively, with the increase of $|\zeta_p|$. This trend is noted to also agree with the prediction of $\mu_{ep}^{(3)}$ in Eq. (3) for low Peclet numbers. It, however, goes against that reported by Vaghef-Koodehi et al. [35], the reason behind which is currently unclear. Overall, our observed buffer concentration, particle size, and particle zeta potential effects on nonlinear electrophoresis are all in good agreement with the prediction of $\mu_{ep}^{(3/2)}$ in Eq. (6). This phenomenon seems to align with our estimated values of Peclet number that are more inclined towards the high regime.

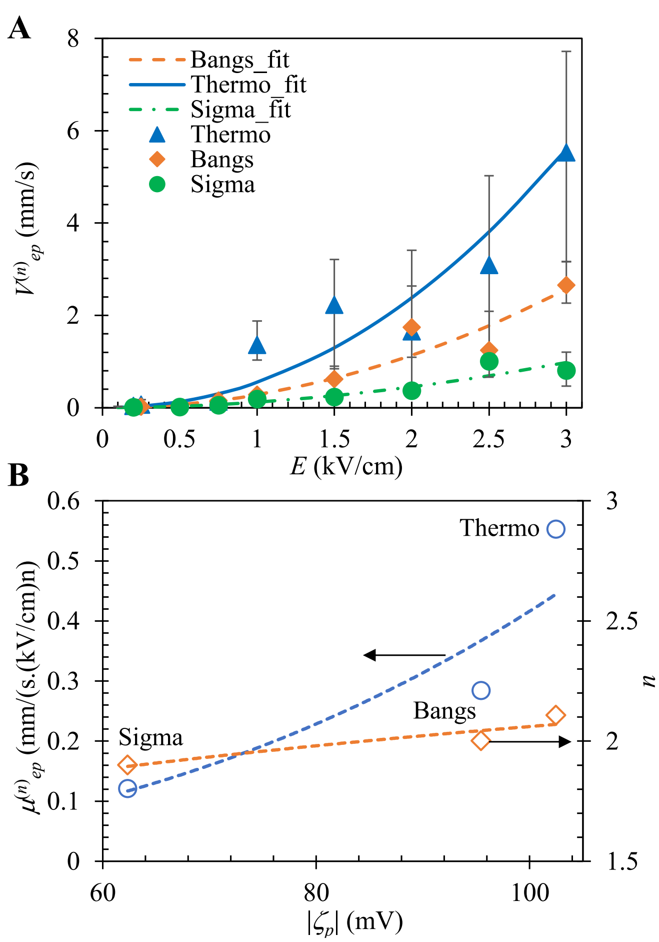

Figure 6. Nonlinear electrophoresis of 5 μm-diameter Thermo-Scientific, Bangs Laboratories and Sigma-Aldrich particles in 0.075 mM buffer solution: (A) Experimentally obtained (symbols with error bars) nonlinear electrophoretic velocity, $V_{ep}^{(n)}$, as a function of electric field, where the curves are the power trendlines best fitted for the experimental data points; (B) Analytically extracted (symbols) nonlinear electrophoretic mobility, $\mu_{EP}^{(n)}$, and nonlinear index, n, from the power trendlines in (A) as a function of the particle zeta potential, $|\zeta_p|$, where the dashed lines are the power fits for the analytical data points.

4 Concluding remarks

We have experimentally studied the effects of buffer concentration, particle size, and particle zeta potential on the nonlinear electrophoresis of polystyrene particles in a straight rectangular microchannel. The measured data for the nonlinear electrophoretic particle velocity as a function of the applied electric field are best fitted with a positive power trendline for each case. The nonlinear electrophoretic particle mobility, $\mu_{ep}^{(n)}$, and nonlinear index, n, extracted from the trendlines are both found to increase with the decrease of buffer concentration and particle size or the increase of particle zeta potential. However, the nonlinear index, n, stays at the value of 2 with a deviation of no more than ±0.5 in all the tested cases, which appears to be within the 3- and 3/2-order dependences for low and high electric fields, respectively. Moreover, the obtained trends for $\mu_{ep}^{(n)}$ as a function of the tested fluid and particle properties are all consistent with the theoretical prediction of $\mu_{ep}^{(3/2)}$ in terms of the Dukhin number. This observation turns out to be in line with our estimated values of Peclet number that are inclined towards the high regime in all cases. For future work, we will study if biological cells experience nonlinear electrophoresis [45] that may be utilized for enhanced detection throughput [46]. We will also look into the influences of other factors on nonlinear particle electrophoresis such as dielectric polarization and hydrophobicity etc. [43,47-50].

This work was supported in part by NSF under grant number CBET-2100772 and CBET-2127825, and by Clemson University through the Creative Inquiry Program.

The authors have declared no conflict of interest.

Data availability statement

The data that support the findings of this study are available from the corresponding author upon reasonable request.

5 References

[1] Xuan, X., *Electrophoresis* 2019, *40*, 2484-2513.

[2] Vaghef-Koodehi, A., Lapizco-Encinas, B. H., *Electrophoresis* 2022, *43*, 263–287.

[3] Diaz-Armas, G. G., Cervantes-Gonzalez, A. P., Martinez-Duarte, R., Perez-Gonzalez, V. H., *Electrophoresis* 2022, *43*, 327–339.

[4] Kang, Y., Li, D., *Microfluid. Nanofluid.* 2009, *6*, 431-460.

[5] Zhao, C., Yang, C., *Microfluid. Nanofluid.* 2012, *13*, 179-203.

[6] Khair, A. S., Posluszny, D. E., Walker, L. M., *Phys. Rev. E* 2012, *85*, 016320.

[7] Zhao, C., Yang, C., *Adv. Colloid. Interface Sci.* 2013, *201-202*, 94-108.

[8] Hunter, R. J., *Zeta potential in colloid science*, Academic Press, New York 1981.

[9] Masliyah, J. H., Bhattacharjee, S., *Electrokinetic and Colloid Transport Phenomena*, Wiley-Interscience 2006.

[10] Morrison, F. A., *J. Colloid. Interface Sci.* 1970, *34*, 210-214.

[11] Li, D. *Electrokinetics in microfluidics*, Elsevier Academic Press, Burlington, MA 2004.

[12] Lyklemma, J., *Fundamentals of Interface and Colloid Science*, Academic Press 1991.

[13] Dukhin, S. S., *Adv. Colloid Interface Sci.* 1993, *44*, 1-134.

[14] Chang, H. C., Yeo, L. Y., *Electrokinetically Driven Microfluidics and Nanofluidics*, Cambridge University Press, New York 2010.

[15] O'Brien, R. W., White, L. R., *J. Chem. Soc. Faraday Trans.* 1978, *74*, 1607-1626.

[16] Dukhin, S. S., Shilov, V. N., *Adv. Colloid Interface Sci.* 1980, *13*, 153–195.

[17] O'Brien, R. W., *J. Colloid Interface Sci.* 1983, *92*, 204-216.

[18] Schnitzer, O., Yariv, E., *Phys. Rev. E* 2012, *86*, 021503.

[19] Dukhin, S. S., *Adv. Colloid Interface Sci.* 1991, *36*, 219-248.

[20] Mishchuk, N. A., *Adv. Colloid Interface Sci.* 2010, *160*, 16-39.

[21] Schnitzer, O., Zeyde, R., Yavneh, I., Yariv, E., *Phys. Fluids* 2013, *25*, 052004.

[22] Sherwood, J. D., Ghosal, S., *J. Fluid. Mech.* 2018, *843*, 847-871.

[23] Schnitzer, O., Yariv, E., *Phys. Fluids* 2014, *26*, 122002.

[24] Mishchuk, N. A., Dukhin, S. S., *Electrophoresis* 2002, *23*, 2012–2022.

[25] Shilov, V., Barany, S., Grosse, C., Shramko, O., *Adv. Colloid Interface Sci.* 2003, *104*, 159–173.

[26] Khair, A. S., *Current Opinion Colloid Interface Sci.* 2022, *59*, 101587.

[27] Kontush, S. M., Dukhin, S. S., Vidov, O. I., *Kolloidnyi Zh.* (in Russian) 1994, *56*, 654–660.

[28] Barany, S., *Adv. Colloid Interface Sci.* 2009, *147–148*, 36–43.

[29] Mishchuk, N. A., Barinova, N. O., *Colloid J.* 2011, *73*, 88–96.

[30] Youssefi, M. R., Diez, F. J., *Electrophoresis* 2016, *37*, 692.

[31] Tottori, S., Misiunas, K., Keyser, U. F., *Phys. Rev. Lett.* 2019, *123*, 014502.

[32] Cardenas-Benitez, B., Jind, B., Gallo-Villanueva, R. C., Martinez-Chapa, S. O., Lapizco-Encinas, B. H., Pérez-González, V. H., *Anal. Chem.* 2020, *92*, 12871−12879.

[33] Coll De Peña, A., Miller, A., Lentz, C. J., Hill, N., Parthasarathy, A., Hudson, A. O., Lapizco-Encinas, B. H., *Anal. Bioanal. Chem.* 2020, *412*, 3935–3945.

[34] Antunez-Vela, S., Perez-Gonzalez, V. H., De Peña, A. C., Lentz, C. J., Lapizco-Encinas, B. H., *Anal. Chem.* 2020, *92*, 14885–14891.

[35] Vaghef-Koodehi, A., Dillis, C., Lapizco-Encinas, B. H., *Anal. Chem.* 2022, *94*, 6451-6456.

[36] Ruz-Cuen, R., de los Santos-Ramírez, J. M., Cardenas-Benitez, B., Ramírez-Murillo, C. J., Miller, A., Hakim, K., Lapizco-Encinas, B. H., Perez-Gonzalez, V. H., *Lab Chip*, 2021, *21*, 4596-4607.

[37] Zhu, J., Xuan, X., *Electrophoresis* 2009, *30*, 2668-2675.

[38] Yan, D., Yang, C., Huang, X., *Microfluid. Nanofluid.* 2007, *3*, 333-340.

[39] Xuan, X., *Electrophoresis* 2021, *43*, 167–189. https://doi.org/10.1002/elps.202100090

[40] Xuan, X., *Electrophoresis* 2008, *29*, 33-43.

[41] DGT Research, https://www.dgtresearch.com/diffusion-coefficients/.

[42] Kirby, B. J., Hasselbrink Jr., E. F., *Electrophoresis* 2004, *25*, 203-213.

[43] Schnitzer, O., Yariv, E., *Phys. Fluids* 2012, *24*, 082005.

[44] Sze, A., Erickson, D., Ren, L., Li, D., *J. Colloid Interface Sci.* 2003, *261*, 402–410.

[45] Li, N., Wang, P., Wang, S., Wang, C., Zhou, H., Kapur, S., Zhang, J., Song, Y., *J. Environ. Chem. Eng.* 2022, *10*, 107516.

[46] Hou, T., Chang, H., Jiang, H., Wang, P., Li, N., Song, Y., Li, D., *Measurement* 2022, *187*, 110304.

[47] Yossifon, G., Frankel, I., Miloh, T., *Phys. Fluids* 2007, *19*, 068105.

[48] Yariv, E., Davis, A. M. J., *Phys. Fluids* 2010, *22*, 052006.

[49] Bhattacharyya, S., De, S., *Phys. Rev. E* 2015, *92*, 032309.

[50] Bhattacharyya, S., Majee, P. S., *Phys. Rev. E* 2017, *95*, 042605.